Seismic Performance of a Self-Centering Steel Moment Frame Building

Presentation · June 2018

CITATIONS
0

READS
259

3 authors:

Xingquan Guan
University of California, Los Angeles
10 PUBLICATIONS **63** CITATIONS
SEE PROFILE

Saber Moradi
Ryerson University
28 PUBLICATIONS **199** CITATIONS
SEE PROFILE

Henry Burton
University of California, Los Angeles
50 PUBLICATIONS **323** CITATIONS
SEE PROFILE

Eleventh U.S. National Conference on Earthquake Engineering
Integrating Science, Engineering & Policy
June 25-29, 2018
Los Angeles, California

SEISMIC PERFORMANCE OF A SELF-CENTERING STEEL MOMENT FRAME BUILDING

X. Guan[1], S. Moradi[2] and H. Burton[3]

ABSTRACT

This paper studies the seismic performance of a self-centering moment resisting frame (SC-MRF) using post-tensioned (PT) PT connections with top-and-seat angles. A phenomenological model that captures lateral load response and collapse behavior of PT connections is developed and then verified using previous experiments. To study the seismic performance of SC-MRFs, a prototype building, which has SC-MRFs as its lateral force resisting system, is considered for the analytical modeling. A 2D OpenSees model for the SC-MRF is built by using the developed phenomenological model. A conventional welded MRF (WMRF) model, which has the same member sizes is also created. Finally, monotonic pushover analysis and incremental dynamic analysis are performed on both SC-MRF and WMRF models. The static analysis results indicate that the static strength of the SC-MRF is 40% lower than that of the WMRF. The fragility results show that the WMRF has higher collapse resistance, whereas the SC-MRF undergoes smaller residual drift.

[1]Graduate Student Researcher, Dept. of Civil and Environmental Engineering, University of California, Los Angeles, 2541 Boelter Hall, Los Angeles, CA 90095 (email: guanxingquan@ucla.edu)
[2]Assistant Professor, Dept. of Civil Engineering, Ryerson University, Toronto, Ontario, M5B 2K3 (email: s.moradi@ryerson.ca)
[3]Assistant Professor, Dept. of Civil and Environmental Engineering, University of California, Los Angeles, 5731H Boelter Hall, Los Angeles, CA 90095 (email: hvburton@ucla.edu)

Seismic Performance of a Self-Centering Steel Moment Frame Building

X. Guan[1], S. Moradi[2] and H. Burton[3]

ABSTRACT

This paper studies the seismic performance of a self-centering moment resisting frame (SC-MRF) using post-tensioned (PT) PT connections with top-and-seat angles. A phenomenological model that captures lateral load response and collapse behavior of PT connections is developed and then verified using previous experiments. To study the seismic performance of SC-MRFs, a prototype building, which has SC-MRFs as its lateral force resisting system, is considered for the analytical modeling. A 2D OpenSees model for the SC-MRF is built by using the developed phenomenological model. A conventional welded MRF (WMRF) model, which has the same member sizes is also created. Finally, monotonic pushover analysis and incremental dynamic analysis are performed on both SC-MRF and WMRF models. The static analysis results indicate that the static strength of the SC-MRF is 40% lower than that of the WMRF. The fragility results show that the WMRF has higher collapse resistance, whereas the SC-MRF undergoes smaller residual drift.

Introduction

In current seismic design codes, structures are designed to achieve a goal of collapse prevention. This requires that structures have sufficient ductility to resist earthquake loading. As a result, conventional steel structures normally undergo permanent deformations (or so-called residual deformation) after earthquakes. The residual deformation becomes a major concern since it significantly increases the repair cost. Large permanent deformations make the building repair work prohibitive.

With the goal of minimizing residual deformations, researchers investigate the applications of new materials [1-3]. However, these systems require new materials and/or special structural systems that can make them less practical. An efficient approach to achieve this goal is to use post-tensioned (PT) connections with top-and-seat angles [4, 5]. Fig. 1 shows schematic views of conventional and PT connections. In a PT connection, PT strands are used to provide restoring forces while energy dissipation elements (such as top-and-seat angles) are incorporated to dissipate energy. As a result, structural damage in the connection is localized to the angles, which can be easily replaced following earthquakes.

To assess the advantages of using self-centering moment resisting frames (SC-MRFs)

[1]Graduate Student Researcher, Dept. of Civil and Environmental Engineering, University of California, Los Angeles, 2541 Boelter Hall, Los Angeles, CA 90095 (email: guanxingquan@ucla.edu)
[2]Assistant Professor, Dept. of Civil Engineering, Ryerson University, Toronto, Ontario, M5B 2K3 (email: s.moradi@ryerson.ca)
[3] Assistant Professor, Dept. of Civil and Environmental Engineering, University of California, Los Angeles, 5731H Boelter Hall, Los Angeles, CA 90095 (email: hvburton@ucla.edu)

with PT connections, the seismic performance of these new systems should be studied. To achieve this goal, a reliable modeling technique that can capture the collapse behavior of PT connection is necessary. However, the existing modeling methods are mainly focused on PT connections with other types of energy dissipation devices, such as web hourglass shape steel [6], friction devices [7], and passive dampers [8]. It is thus of great importance to develop a reliable modeling technique for PT connections with top-and-seat angles, thereby predicting the structural response of SC-MRFs subjected to earthquake loading.

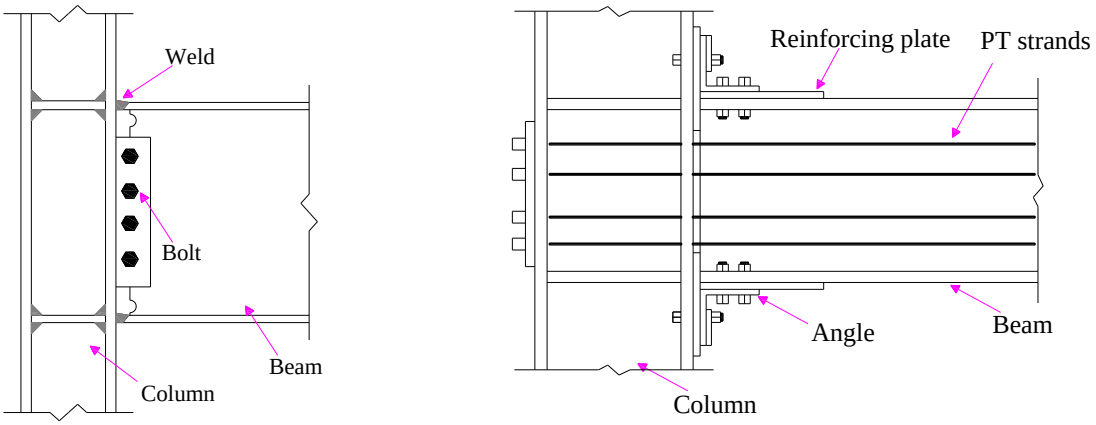

(a) Conventional welded connection (b) PT connection

Figure 1. Elevation view of welded connection and PT connection.

In this study, a phenomenological model of PT connections is developed in OpenSees [9] and the model is subsequently verified using previous experiments. A prototype building, which has SC-MRFs as its lateral force resisting system, is selected. A 2D model for the SC-MRF is built based on the proposed phenomenological model. Finally, static pushover and dynamic analyses are conducted to study the lateral load carrying capacity and collapse resistance of PT connections with bolted angles. The performance of SC-MRFs is also compared with that of conventional welded MRFs (WMRFs).

Model Development in OpenSees

Description of Prototype Building

A 6-story, 6-bay by 6-bay office building reported by Garlock et al. [10] is selected as the prototype building. The building, located in the Los Angeles area, has two identical MRFs to resist lateral loads in both E-W and N-S directions. One of these four MRFs is chose for the current study. The frame is designed as an SC-MRF using PT connections with top-and-seat angles based on the methodology proposed by Garlock et al. [10]. The detailed information about the SC-MRF, such as member sizes, connection details, and geometric dimensions can be found in the reference [10].

Component-level Modeling

Phenomenological Model of PT Connection

A phenomenological model of the PT connection is developed in OpenSees, as shown in Fig. 2. Mechanical behavior of a PT connection is governed by two main components: PT strands and top-and-seat angles. The PT strands provide restoring force whereas the angles dissipate energy. Therefore, in the modeling, two materials, acting in parallel are defined: "self-centering" and "pinching4" materials. The former represents the PT strands and the latter represents the angles. Then the parallel material is assigned to a rotational spring. The beams and columns are modeled using elastic beam-column elements. The column hinge is modeled using a rotational spring with modified IMK material.

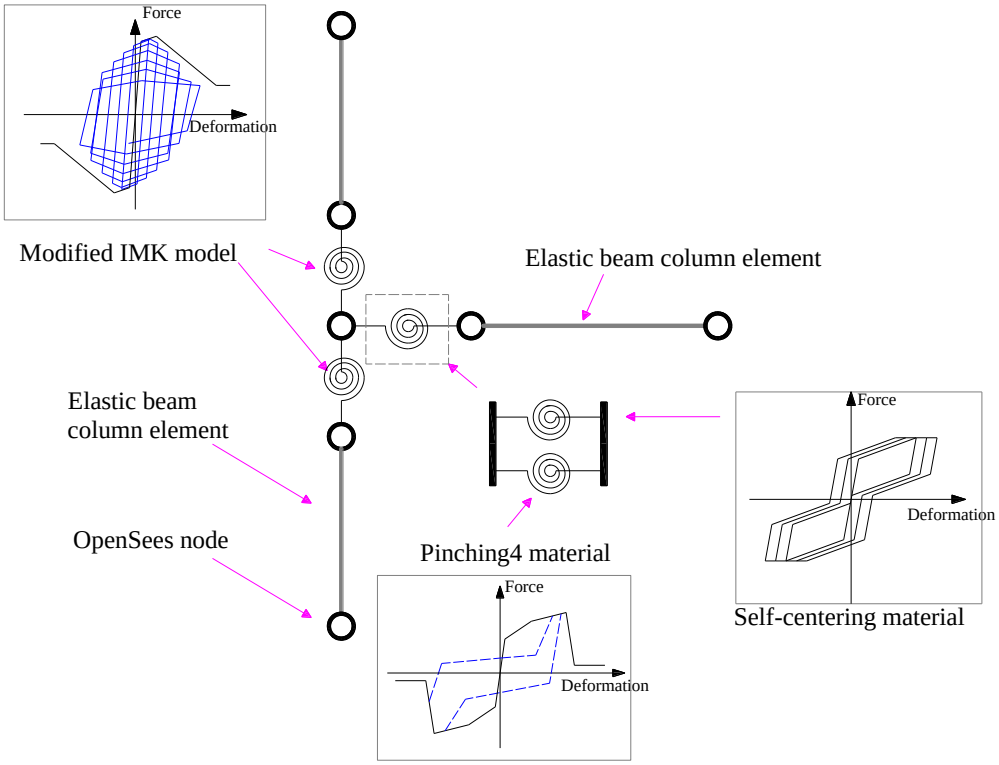

Figure 2. Model for an exterior PT connection with top-and-seat angles.

Validation of the Proposed Model

To assess the capability of the phenomenological model for capturing the cyclic response of PT connections, the analytical lateral load-displacement response is compared to existing experimental data for a number of PT connections. Specimens *PC2*, *PC3*, *PC4*, and *20s-18* reported in references [4, 5] are selected for the validation of the modeling in this study. In the analytical models, the lengths for the beams and columns are set as the actual values measured from the experiments. The parameters for the self-centering and pinching4 materials are determined using an iterative process. In this process, the experimental cyclic loading protocol is applied to the model and the parameters relating to the material are adjusted until observing a good match between the simulated and experimental hysteretic curves. Fig. 3 illustrates a comparison between the analytical and experimental results for the four specimens. The plots show that the analytical results match well with experimental results; therefore, the proposed model is capable of predicting the response of PT connections.

Calibration of PT connections in the Prototype Building

The PT connections in the SC-MRF of the prototype building can be modeled using the proposed modeling. In the absence of experimental data on the lateral response of PT connections of varied geometric details, the empirical equations developed by Moradi [11] are used to determine backbone curve parameters, including initial stiffness, gap-opening point, hardening stiffness, and ultimate strength for PT connections. The empirical equations can predict the lateral load-drift response and the limit state behavior of PT connections [12]. The empirical equations have been developed considering different damage states including beam local buckling, angle fracture, strand fracture, and excessive yielding of tensile bolts in PT connections. In the current study, a post-peak slope of -0.167 is considered based on the average of values from the experimental response [4]. The residual strength is assumed to be 40% of the maximum strength. With the empirical equations, post-peak slope, and residual strength, complete backbone curves can be drawn. The PT connections in the prototype building are then calibrated based on the generated backbone curves. Fig. 4 shows typical calibration results of the PT connection on the 1st floor of the SC-MRF. The detailed parameters for all the PT connections are summarized in Tables 1 and 2. The definition of variables in these two tables can be found in the OpenSees manual [9].

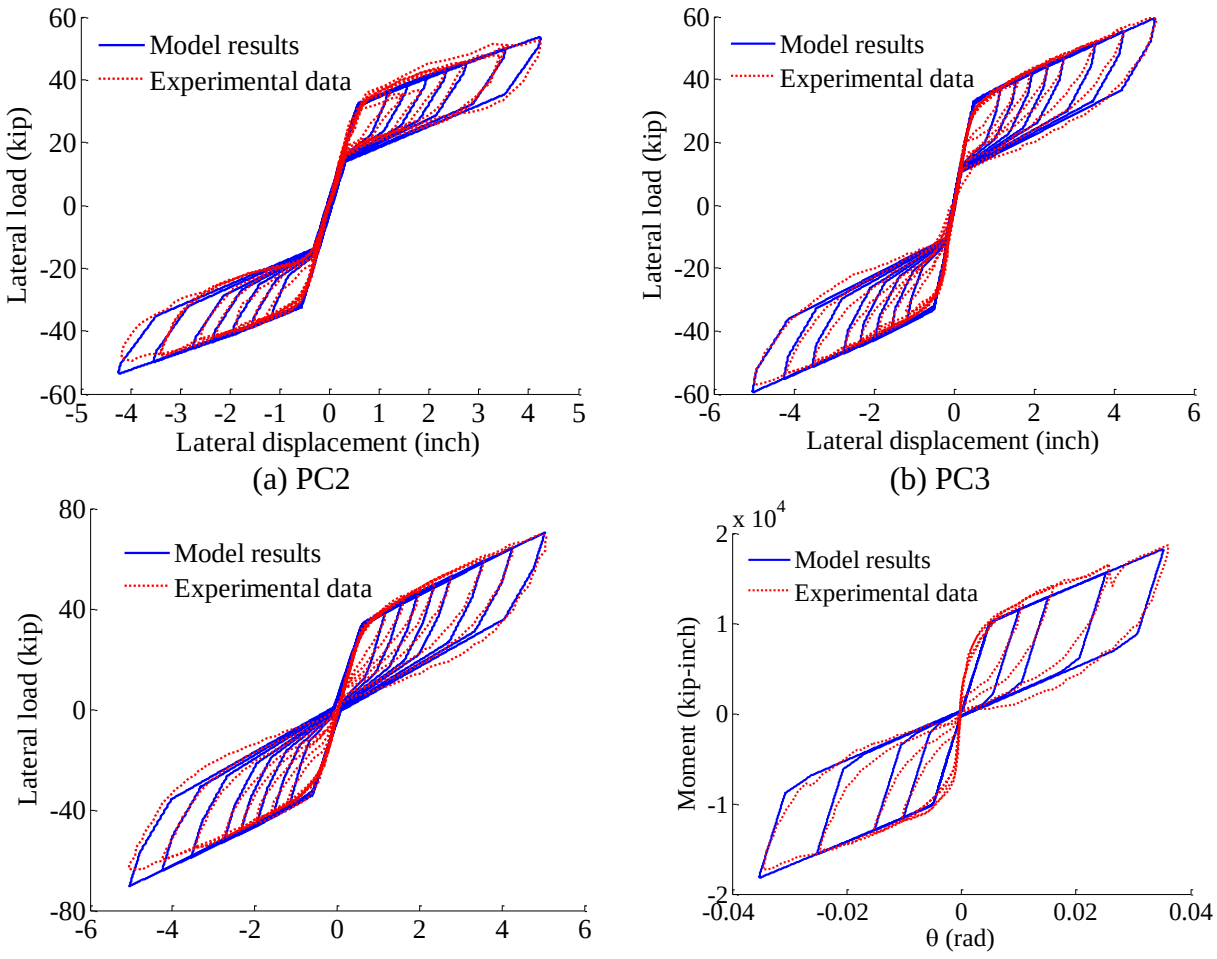

Figure 3. Comparison between proposed model and experimental data (adapted from [4, 5]).

Structural Modeling

A 2D analysis model is developed for the SC-MRF in the prototype building by using the PT connection models described earlier, i.e., elastic beam-column elements for beams and columns, rotational springs with modified IMK model for column hinges, and rotational springs with self-centering and pinching4 material in parallel. Additionally, panel zones are explicitly modeled using the approach reported in reference [13]. A leaning column is modeled to account for second-order P-Δ effects. The mass on each floor is lumped at the nodes on the leaning column. Fig. 5 shows the OpenSees model for the SC-MRF.

Table 1. Parameters for self-centering material of PT connections

Floor No.	Self-centering material			
	k1 (kip-inch/rad)	k2 (kip-inch/rad)	sigAct (kip-inch)	β
1	1.00E+07	1.00E+05	1.60E+04	0.75
2	1.00E+07	1.00E+05	1.60E+04	0.75
3	1.00E+07	1.00E+05	1.40E+04	0.75
4	1.40E+07	8.00E+04	1.20E+04	0.75
5	1.00E+07	6.00E+04	1.20E+04	0.75
6	1.00E+07	4.00E+04	5.00E+03	0.75

Table 2. Parameters for pinching4 material of PT connections

Floor No.	Pinching4 material							
	ePf1 (kip-inch)	ePf2 (kip-inch)	ePf3 (kip-inch)	ePf4 (kip-inch)	ePd1 (rad)	ePd2 (rad)	ePd3 (rad)	ePd4 (rad)
1	1.23E+03	3.00E+04	6.50E+04	-4.00E+04	0.0008	0.01	0.03	0.07
2	1.20E+03	1.80E+04	4.20E+04	-4.70E+04	0.0005	0.01	0.025	0.07
3	9.00E+02	1.50E+04	3.90E+04	-4.00E+04	0.0005	0.01	0.0265	0.065
4	4.50E+02	1.25E+04	2.90E+04	-3.10E+04	0.0005	0.01	0.024	0.065
5	4.50E+02	1.22E+04	3.20E+04	-3.00E+04	0.0005	0.01	0.026	0.07
6	2.25E+02	7.00E+03	1.75E+04	-1.40E+04	0.0005	0.01	0.025	0.066

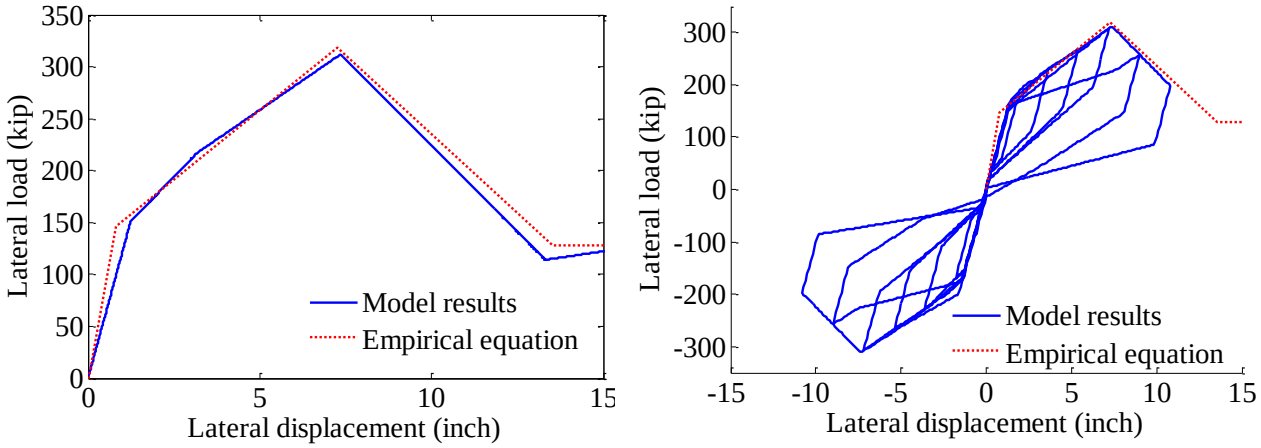

(a) Monotonic loading (b) Cyclic loading

Figure 4 Calibration of PT connection model on 1st floor (empirical equation from [11])

A 2D model for WMRF is also built. To provide a basis for comparisons, the WMRF has the same member sizes as in the SC-MRF. Therefore, the WMRF and SC-MRF have similar periods of vibration. Except the beam hinges, the modeling of the WMRF is similar to that for the SC-MRF. In the WMRF model, the beam hinge is modeled as a rotational spring with modified IMK material instead of self-centering and pinching4 materials in parallel.

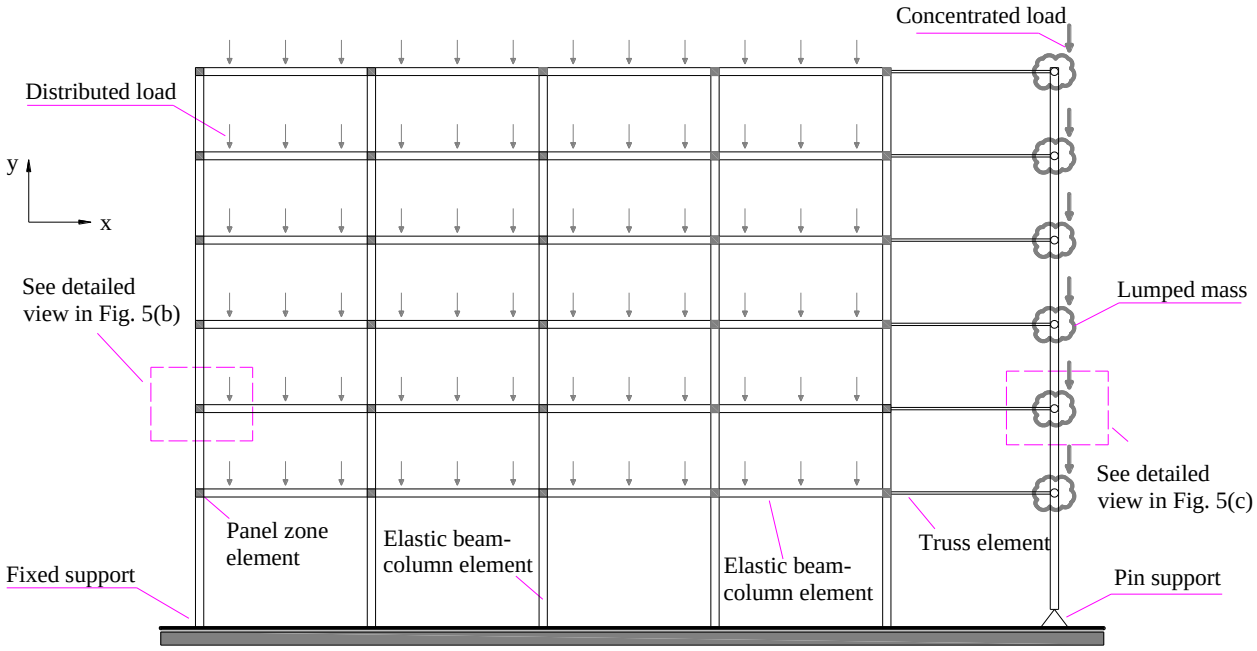

(a) Overview of 2D OpenSees model

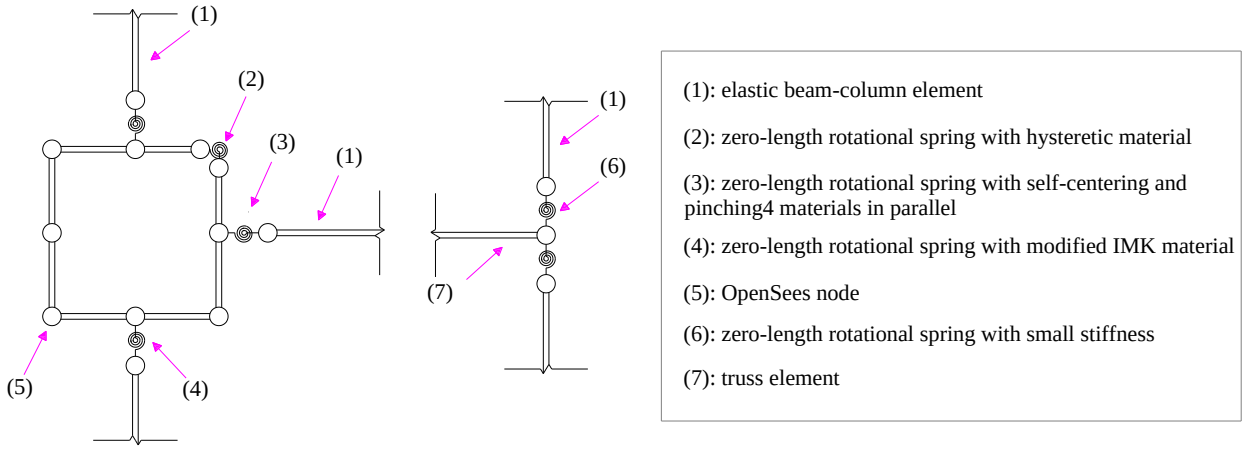

(b) Details for SC-MRF connection (c) Details for leaning column joint

Figure 5. OpenSees model for SC-MRF

Nonlinear Static and Dynamic Analysis

Static Pushover Response

Monotonic static pushover analysis is performed on both SC-MRF and WMRF models using the

lateral loading pattern prescribed in ASCE 7-10 [14]. Fig. 6 shows the static pushover responses for the SC-MRF and WMRF models. The static strength of the SC-MRF is 40% lower than that of the WMRF. However, its strength degrades more gradually. Additionally, both frame models have an identical initial stiffness. These observations can be explained by the mechanical behavior of the different types of connections used in the frame. Fig. 7 shows the comparison of the backbone curves for the PT connection and conventional welded connections. The peak strength of the welded connection is higher than that of the PT connection. Moreover, both connections have similar initial stiffness. These observations are consistent with those from Fig. 6.

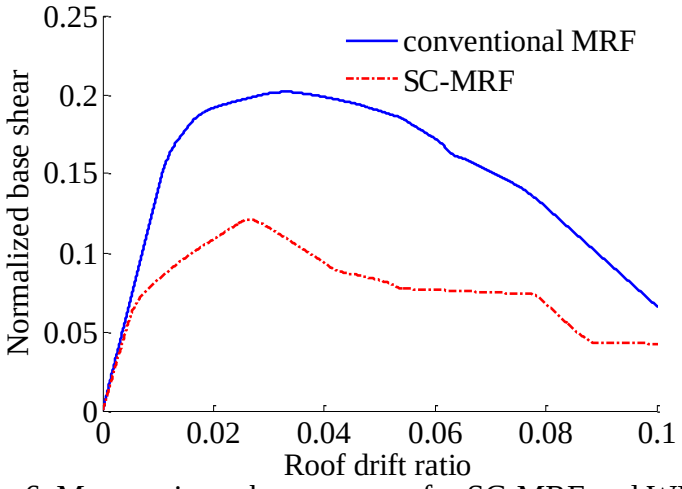

Figure 6. Monotonic pushover curves for SC-MRF and WMRF.

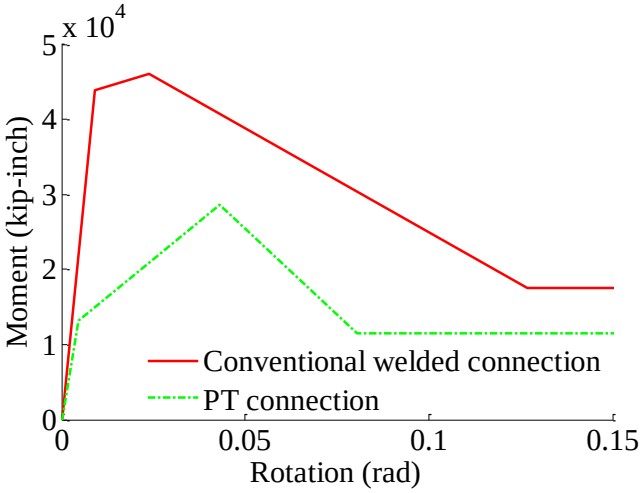

Figure 7. A typical comparison of backbone curves between PT and welded connections.

Incremental Dynamic Analysis and Fragility Curves

The dynamic performance of the SC-MRF and WMRF is assessed using the incremental dynamic analysis (IDA) technique. Nonlinear dynamic analyses are performed by using 44 far-field ground motions and the scaling method of FEMA P695 [15]. The OpenSees structural model is capable to simulate the flexural strength and stiffness deterioration of the beams and

columns, which are significantly influencing the collapse behavior of the buildings. Based on the IDA analysis, the fragility functions are estimated using the maximum likelihood method specified in reference [16]. Fragility functions are probabilistic distributions used to quantify the probability that the structure will be damaged as a function of an intensity measure or engineering demand parameter.

Fig. 8(a) shows the collapse fragility curves for both SC-MRF and conventional WMRF models based on a maximum drift limit of 10%. The collapse probabilities are shown as a function of the spectral acceleration at 1st mode period of the structure (S_a). The intensities at 50% probability of collapse for the SC-MRF and WMRF are 2.03g and 1.07g, respectively, which indicates that the collapse resistance of the WMRF is significantly higher than that of the SC-MRF. Fig. 8(b) shows the demolition fragility curves for both frame models based on a residual drift limit of 0.5%. The intensities at 50% probability of demolition for the SC-MRF and WMRF are 0.67g and 0.57g, respectively, which indicates that the PT connection is efficient in minimizing the residual drift.

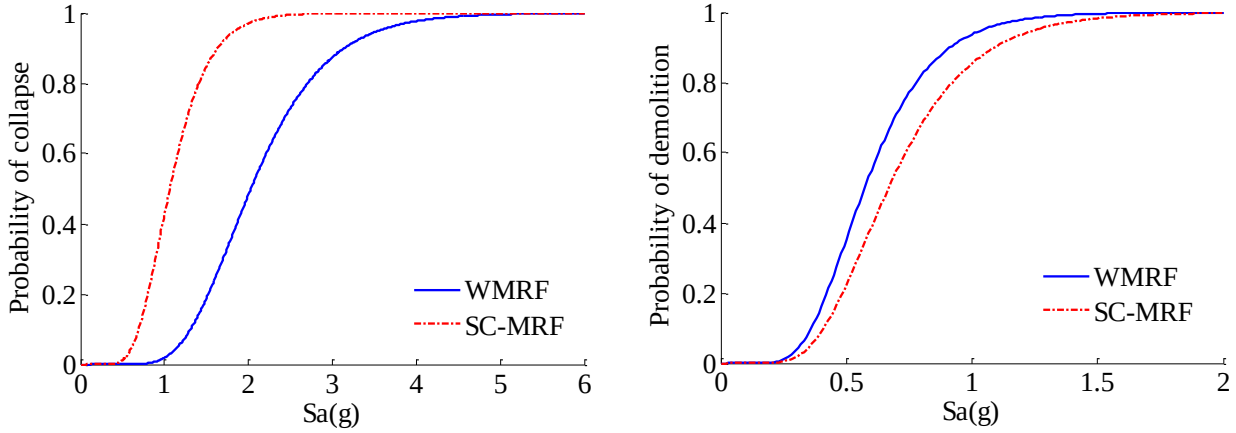

(a) Collapse fragility curves (b) Demolition fragility curves

Figure 8. Fragility results

Conclusions

This paper provides a systematic study on the seismic performance of an SC-MRF in comparison with a conventional WMRF. Firstly, a reliable phenomenological model is developed and verified against past experimental results. Then a prototype building, which has SC-MRFs as its lateral force resisting system, is selected. An OpenSees model is created for the SC-MRF using the proposed phenomenological model for the connections. Static pushover and dynamic analyses are subsequently performed to study the lateral response of the frame models. The analytical results for the SC-MRF are compared with those for the WMRF, which has the same column and beam sizes. The static analysis results indicate that the strength of the SC-MRF is 40% lower than that of the WMRF. The dynamic analysis results indicate that the WMRF has higher collapse resistance, whereas the SC-MRF undergoes smaller residual drift values. To gain a thorough understanding of the seismic performance of SC-MRFs, future research shall be extended to the damage loss assessment for the SC-MRFs using FEMA P58 [17].

References

1. Miller DJ, Fahnestock LA, Eatherton MR. Development and experimental validation of a nickel-titanium shape memory alloy self-centering buckling-restrained brace. *Engineering Structures* 2012; 40: 288-298.
2. Fang C, Yam MCH, Lam ACC, Xie L. Cyclic performance of extended end-plate connections equipped with shape memory alloy bolts. *Journal of Constructional Steel Research* 2014; 94: 122-136.
3. Asgarian B, Moradi S. Seismic response of steel braced frames with shape memory alloy braces. *Journal of Constructional Steel Research* 2011; 67: 65-74.
4. Garlock MM, Ricles JM, Sause R. Experimental studies of full-scale posttensioned steel connections. *Journal of Structural Engineering* 2005; 131(3): 438-448.
5. Ricles JM, Sause R, Peng SW, Lu LW. Experimental evaluation of earthquake resistant posttensioned steel connections. *Journal of Structural Engineering* 2002; 128(7): 850-859.
6. Dimopoulos AI, Karavasilis TL, Vasdravellis G, Uy B. Seismic design, modelling and assessment of self-centering steel frames using post-tensioned connections with web hourglass shape pins. *Bulletin of Earthquake Engineering 2013*; 11(5): 1797-1816.
7. Rojas P, Ricles JM, Sause R. Seismic performance of post-tensioned steel moment resisting frames with friction devices. *Journal of Structural Engineering* 2005; 131(4): 529-540.
8. Dimopoulos AI, Tzimas AS, Karavasilis TL, Vamvatsikos D. Probabilistic economic seismic loss estimation in steel buildings using post-tensioned moment-resisting frames and viscous dampers. *Earthquake Engineering and Structural Dynamics* 2016; 45(11): 1725-1741.
9. Mazzoni S, McKenna F, Scott MH, Fenves GL. The Open System for Earthquake Engineering Simulation (OpenSEES) User command-language manual 2006
10. Garlock MM, Sause R, Ricles JM. Behavior and design of posttensioned steel frame system. *Journal of Structural Engineering* 2007; 133(3): 389-399
11. Moradi S. Simulation, response sensitivity, and optimization of post-tensioned steel beam-column connections. *Doctoral dissertation* 2016; University of British Columbia.
12. Moradi S, Alam MS. Lateral load-drift response and limit states of posttensioned steel beam-column connections: parametric study. *Journal of Structural Engineering* 2017; 143(7): 1-13.
13. Gupta A, Krawinkler H. Seismic demands for the performance evaluation of steel moment resisting frame structures. *Doctoral dissertation* 1999; Stanford University.
14. ASCE. Minimum design loads for buildings and other structures. *ASCE 7-10* 2010; Reston, VA.
15. FEMA. Quantification of building seismic performance factors. *FEMA P695* 2009; Applied Technology Council, Redwood City, CA.
16. Baker JW, Efficient analytical fragility function fitting using dynamic structural analysis. *Earthquake Spectra* 2015; 31(1): 579-599.
17. FEMA. Seismic performance assessment of buildings. *FEMA P58-1* 2012; Applied Technology Council, Redwood City, CA.